

## A Method to Infer the Three Cartesian Wavelengths of a Mountain Wave from Three Soundings

P. ALEXANDER AND A. DE LA TORRE

*Departamento de Física, Facultad de Ciencias Exactas y Naturales, Universidad de Buenos Aires,  
Buenos Aires, Argentina*

(Manuscript received 21 July 2009, in final form 18 March 2010)

### ABSTRACT

The number of atmospheric sounding techniques and the amount of missions within each of them continue to grow at the present time. The probability of having two or more profiles in a given region and time interval therefore is increasing. In the case of three close observations it would be a priori possible to infer the three Cartesian wavelengths of a mountain wave. However, the relative orientation of the three sounding paths cannot be arbitrary and must fulfill some conditions to avoid errors growing out of given bounds.

### 1. Introduction

Buoyancy under stable stratification in the atmosphere provides a restoring force for disturbances from equilibrium, leading to the oscillations represented by a wave field. These perturbations are known as gravity waves. Except at very low intrinsic frequencies (periods of many hours at least), Coriolis force can be ignored. The perturbations are assumed to be perpendicular to the wave vector, so the wave solutions to the governing equations may then be found with the consideration of plane waves in one horizontal and one vertical dimension (see, e.g., Holton 2004), whereby an infinite wavelength is implicitly assumed in the other horizontal direction. Mountain waves (MW) are a particular case of these solutions.

MW are generated by airflow over orography and usually they have null frequency with respect to the underlying terrain. Their frequency in the intrinsic system does therefore not vanish, whereby westerlies (easterlies) make phase fronts propagate to the west (east) in that frame of reference. Since upward propagation of energy requires downward phase propagation, constant phase fronts must tilt westward (eastward) with increasing height above the mountains (see, e.g., Gill 1982). Oscillations can reach the

stratosphere and even go further up amplified by energy density conservation.

Wavelengths inferred from an atmospheric sounding (hereinafter apparent or detected values) are generally not equal to the real (or original) Cartesian values, as the profiles (of whatever atmospheric variable) are usually not obtained on strictly or nearly horizontal or vertical directions. Because essentially all techniques depart from horizontal or vertical sounding lines, the detected wavelengths must be distinguished from the original Cartesian horizontal or vertical ones and appropriately reconstructed according to wave constant phase surfaces' orientation and the sounding direction (a simple two-dimensional example is shown in Fig. 1, where two soundings would be needed to infer the two real wavelengths). Moreover, notice that if by chance a sounding is performed parallel to the wave fronts, then the detected wavelengths will be apparently infinite. Original wavelengths may be smaller or larger than the apparent values according to the relative orientation between profiling and wave fronts. There is a second source of discrepancy between apparent and real Cartesian wavelengths in those techniques that have a sounding time not much less than the wave periods, as the constant phase surfaces will undergo a displacement during the observation time. Shutts et al. (1994) analyzed this kind of problem and suggested that the near-simultaneous release of between three and five radiosondes upstream of mountains could provide a useful method to study orographic waves.

---

*Corresponding author address:* P. Alexander, Departamento de Física, Facultad de Ciencias Exactas y Naturales, Universidad de Buenos Aires, 1428 Buenos Aires, Argentina.  
E-mail: peter@df.uba.ar

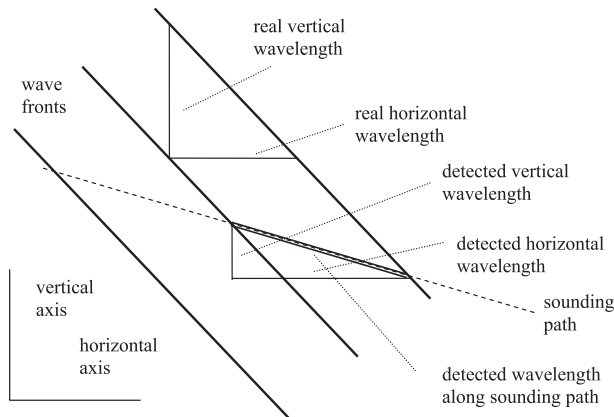


FIG. 1. A 2D diagram showing the possible differences between detected and real wavelengths.

There are a number of works that deal with studies on apparent wavelengths, but they have seldom made any distinction with the real ones, notwithstanding the significant differences that may appear (see, e.g., de la Torre and Alexander 1995; Alexander et al. 2008). Extreme caution must be exerted on conclusions drawn from possibly incomplete information provided by one atmospheric profiling in one direction. The geometrical error source will affect very significantly the MW vertical wavelengths detected from nonvertical profilings, as those are the steepest gravity wave fronts. On the contrary, the nearly horizontal inertio-gravity wave phase planes will lead to the smallest vertical wavelength differences.

The inference of MW wavelengths becomes affected by the discrepancy between detected and real wavelengths but not by the error source due to displacement of the wave fronts during the sounding time, as these waves are usually considered to be stationary with respect to the Earth reference system. It should then be possible a priori to infer the three Cartesian wavelengths (two horizontal and one vertical) of plane MW from three nearby observations in space and time (to make sure they are observing the same atmospheric structure). Measurements are performed nowadays in situ (rockets, balloons, and aircraft) or by remote ground-based (radars and lidars) and space-based methods (satellites). With the presently increasing amount of sources of atmospheric soundings it should be possible in the near future to find increasing quantities of sets of three close measurements observing the same mountain wave. This motivates the development of a method able to extract the original Cartesian wavelengths from the detected ones. Below we intend to develop the method and place the conditions for a successful completion of the inversion problem from apparent to real wavelengths for MW. We first show an example where a high density of satellite soundings during

some months close to a high activity MW region would a priori allow the calculation of the three Cartesian wavelengths in different cases. However, the implementation was not possible as the data did not fulfill the requirements as explained in this work. We were then able to find a successful case by relaxing requirements and with a different combination: two satellite experiments and one balloon sounding.

## 2. The inversion method

The following relation holds for any two points  $\bar{\mathbf{x}}_{a,b}$  on successive fronts of a plane wave represented by a wave vector  $\bar{\mathbf{k}}$ :

$$\bar{\mathbf{k}} \cdot (\bar{\mathbf{x}}_b - \bar{\mathbf{x}}_a) = \pm 2\pi. \quad (1)$$

If we have no a priori information on the wave fronts and their displacement direction we cannot decide which sign applies on the right-hand side of the equation. We will consider that  $\bar{\mathbf{x}}_{a,b}$  are connected by an observational path, which will be considered a straight line. This is often a good representation for many observational techniques. Three independent observations of the wave fronts lead to the following equation set to be solved in order to find the three Cartesian wavelengths  $\lambda_x$ ,  $\lambda_y$ , and  $\lambda_z$ :

$$\begin{aligned} \sin\theta_i \cos\phi_i \frac{1}{\lambda_x} + \sin\theta_i \sin\phi_i \frac{1}{\lambda_y} + \cos\theta_i \frac{1}{\lambda_z} \\ = \pm \frac{1}{\lambda_i} \quad i = 1, 2, 3, \end{aligned} \quad (2)$$

whereby we have expressed the relative position vector  $\bar{\mathbf{x}}_b - \bar{\mathbf{x}}_a$  in each observation in terms of spherical coordinates  $\lambda_i$ ,  $\theta_i$ , and  $\phi_i$ . Notice that  $\lambda_i$  is the wavelength in the direction  $\theta_i$ ,  $\phi_i$  as obtained from a Fourier or any similar analysis on data (it is the detected wavelength along each of the three sounding paths as shown in Fig. 1). The three measurement directions will generally not correspond to an orthogonal base. To evaluate if our wavelength inversion process is well or ill conditioned (that is to say, if small changes in the input will produce small or large changes in the output), we must calculate the condition number  $\kappa(\mathbf{A})$  of the matrix corresponding to the transformations described by the above equation set  $\mathbf{Ax} = \mathbf{b}$  (Press et al. 1999). Then (Golub and Loan 1996)

$$\epsilon_x \leq \frac{\kappa(\mathbf{A})}{1 - \kappa(\mathbf{A})\epsilon_{\mathbf{A}}} (\epsilon_{\mathbf{A}} + \epsilon_{\mathbf{b}}), \quad (3)$$

where  $\epsilon_x$ ,  $\epsilon_{\mathbf{A}}$ , and  $\epsilon_{\mathbf{b}}$  refer to the relative error of  $\mathbf{x}$ ,  $\mathbf{A}$ , and  $\mathbf{b}$ , respectively. The relation bounds the maximum amount of magnification in the relative error of the input that may

be propagated to the solution. For example, let us assume 5% on  $\epsilon_b$  and  $\epsilon_A$  negligible and a condition number value of 6. Then, a 30% uncertainty would follow for the inversion outcome. This simple example shows that it is very difficult to obtain small uncertainties. Position errors of the observations are usually at the meter level (see below), so uncertainties on  $\epsilon_A$  and  $\epsilon_b$  are rather probably related to the representation of the observational path by a straight line, which must be estimated in each case. Evaluations in a real example will be given below, which will show that large uncertainties on the outcome may typically emerge.

One may be tempted to try to find some inequality where an upper bound estimation of the condition number depends on the determinant of  $\mathbf{A}$ , but this is generally not possible. However, we now resort to a result that will allow us to do so in our particular analysis. If each row (or column) of a coefficient matrix is a unit vector in the Euclidean norm, it is said to be equilibrated. The matrix  $\mathbf{A}$  satisfies this requirement for each row. For a non-singular equilibrated matrix it has been shown that

$$\kappa < 2/|d|, \quad (4)$$

where  $|d|$  is the absolute value of the determinant (Guggenheimer et al. 1995). This avoids the need for the computation of the condition number of the configuration, which may be quite a bit more computationally expensive than the calculation of the determinant. We immediately obtain an intuitive result: accuracy is optimal if soundings are mutually perpendicular (determinant of the equilibrated matrix is 1) and becomes very bad if any two experiments are nearly parallel (determinant of the equilibrated matrix is nearly zero). As the determinant of a matrix formed by three unit vectors  $\mathbf{u}_i$  may be written as  $d = (\mathbf{u}_1 \times \mathbf{u}_2) \cdot \mathbf{u}_3 = \sin\alpha \cos\beta$  ( $\alpha$  is the angle between the first two vectors and  $\beta$  the angle between the last vector and the line perpendicular to the plane defined by the former two), we may represent the condition number upper bound in terms of these angles. A similar criterion (there may be just a sign change) applies for any permutation of the vectors. In Fig. 2 we show the condition number upper bound dependency for any given observational configuration. We recall that for negligible error in  $\mathbf{A}$  the uncertainty percentage of the solution may be obtained after multiplying the condition number by the uncertainty percentage of the input [see inequality (3)]. For small  $\alpha$  and for  $\beta$  approaching  $\pi/2$  the upper bound grows out of limit. One case as explained below has been marked in the plot.

It is not possible only with limb observations to form a nearly orthogonal set, because none of them has at least an almost vertical trajectory. However, configurations

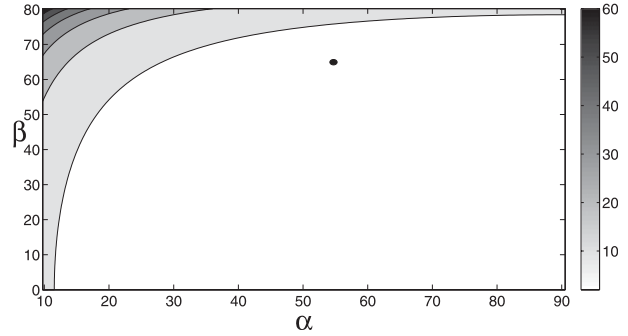


FIG. 2. The condition number upper bound in terms of  $\alpha$  and  $\beta$ . The location on the plane of the analyzed case with one balloon sounding and two global positioning system radio occultations is exhibited as a black dot.

with low error limits may still be found. The determinant of  $\mathbf{A}$  after some algebra may be written as

$$\begin{aligned} d = & \sin\theta_1 \sin\theta_2 \cos\theta_3 \sin(\phi_2 - \phi_1) \\ & + \sin\theta_1 \cos\theta_2 \sin\theta_3 \sin(\phi_1 - \phi_3) \\ & + \cos\theta_1 \sin\theta_2 \sin\theta_3 \sin(\phi_3 - \phi_2). \end{aligned} \quad (5)$$

If  $\theta_i$  are all three similar and close to  $\pi/2$  (limb observations), we may approximate

$$\begin{aligned} d \approx & (\pi/2 - \theta)[\sin(\phi_2 - \phi_1) + \sin(\phi_1 - \phi_3) \\ & + \sin(\phi_3 - \phi_2)]. \end{aligned} \quad (6)$$

So we are led to the following question: what combination of  $\phi_i$  leads to the maximum values of  $|d|$ ? As the third phase is a combination of the former two we must find the maximum for a function  $y$  of two variables  $\gamma$  and  $\delta$ :

$$y = \sin\gamma + \sin\delta + \sin(-\gamma - \delta). \quad (7)$$

The answer is  $\gamma = \delta = 2/3\pi$ . For limb soundings where  $\theta_i = 75^\circ$ , Eqs. (4) and (5) give an upper bound of  $\kappa = 3.2$ , which may lead to reasonable error limits in inequality (3). Notice from the assumptions used in obtaining Eq. (6), that the conclusions on the azimuthal angles may break down if the zenith angles are not similar or if they deviate significantly from limblike methods.

If no further information is added to the problem, then we are led to eight systems (due to the plus-or-minus operator) of three linear equations, without knowing which one to solve. We now use the fact that the tilt of MW vector and fronts may be known according to the forcing wind as mentioned above. For example, the Andes Mountains at midlatitudes in the Southern Hemisphere represent a very important obstacle to the intense westerlies blowing from the Pacific Ocean, generating large-amplitude gravity waves. This north-south (N-S) barrier

(tops around 7 km) generates mountain waves, whose phase surfaces are aligned nearly parallel to the mountains in the N–S direction. We take west–east direction as  $x$ , N–S as  $y$ , and  $z$  is the vertical coordinate. In our example we know that our solutions must comply with  $\lambda_x < 0$  and  $\lambda_z < 0$ . As  $\lambda_y$  is expected to be very large we may ask for  $|\lambda_y| > 3|\lambda_x|$ . No condition exists on the sign of  $\lambda_y$ . We cannot discard that there may be more than one or no acceptable solution for  $\lambda_y$ .

### 3. Discussion of applicability

A global positioning system (GPS) radio occultation (RO) occurs whenever a transmitter on board a satellite from the GPS network at an altitude about 20 000 km rises or sets from the standpoint of a low Earth orbit (LEO) satellite receiver at a height about 800 km and the ray traverses the atmospheric limb. Constellation Observing System for Meteorology, Ionosphere and Climate (COSMIC) is a 6-LEO satellite constellation, launched in April 2006, that performs a larger amount of RO per day than any previous mission (Liou et al. 2007). We tried to take advantage of the anomalously high density of COSMIC RO during the initial mission months at the eastern side of the highest Andes Mountains. Different studies (see, e.g., Preusse et al. 2002) have shown a significant wave activity in the upper troposphere and lower stratosphere in this region.

The aim of GPS RO is to detect the perturbation in Doppler frequency produced by refractive bending of the signal in the limb path between the transmitter and the receiver. The advantages as compared to other methods are that this technique is nearly an instantaneous snapshot (typically 1 min as compared to the much longer atmospheric processes), it has a global coverage, subkelvin accuracy in temperature measurements from the upper troposphere to the lower stratosphere, and it is not interrupted by clouds or weather conditions. However, waves may be overlooked or may appear attenuated because the outcome of this technique depends on the relative orientation between waves and sounding direction. We will just mention two examples: 1) The successive lines of sight between transmitter and receiver may be parallel to the horizontal component of the plane wave vector, and in this case only a weak signature, if any, could be detected (the integrated measure along the ray path will tend to be canceled out by successive positive and negative contributions of the wave); and 2) the successive lines of sight and measurement points could be contained in a wave front, so no changes at all would then be detected.

Within the COSMIC high-density region mentioned above, de la Torre and Alexander (2005) found that the

area 30°–40°S, 70°–65°W showed particularly significant values. From 669 profiles obtained by COSMIC between April 2006 and July 2007 in this zone, 50 pairs of them occurring within 2 h and 200 km of one another were found. From the RO of the 50 pairs it was possible to form 8 triads that satisfied the same spatial and time criteria. The amount of close encounters diminished with time. Although the number of successful occultations rose from about 200 to about 2000 per day over the globe during the 22 considered months, 42 occultation pairs and 8 triads were found between April and December 2006, whereas only 8 pairs and 0 triads were found between January and July 2007. We have chosen to analyze those 8 triads.

To ensure the straight line path requirement we suggest (i) decomposing each observational path on three perpendicular planes and (ii) verifying if the absolute value of the linear correlation coefficient calculated with the points of each of the three decompositions is larger than 0.9. Among the 23 RO of the 8 triads (there were 23 and not 24 RO because one of them was useful for 2 triads), 6 belonging to 3 triads did not survive the straight line sounding test, which led to the calculation of the condition number for 5 triads. All condition numbers were well above 1000. This would amplify the errors in the profiles to significantly large values. It may be seen that three independent occultation observations may not be appropriate to infer the three Cartesian wavelengths. In the present case, the problem was related to the fact that the three RO of each of the triads here considered had similar orientations, which leads to significant error propagation in the linear equation system to be solved (see above). If any two sounding directions are nearly parallel or any sounding direction is a linear combination of the other two, then essentially we have a two-dimensional problem (this will lead to a determinant around zero). The ideal case is when the three soundings are orthogonal among them, as the condition number attains then its lowest value, which is 1, and the error propagation preserves the input relative error. The high density of GPS RO was due to the close position of some LEO satellites during the initial mission months and that they were therefore producing RO with the same GPS satellite (see the details on the initial constellation configuration by Liou et al. 2007). This led in each triad to three close independent profilings, but all of them nearly parallel. Therefore, a high density of observations is not a sufficient condition for a three-dimensional reconstruction of a plane MW structure. Measurement directions must be rather isotropically distributed (see above). It may be more appropriate in the future to combine the continuously increasing number of limb observations like GPS RO from different missions. It may be also possible to complement one or two of them with measurements

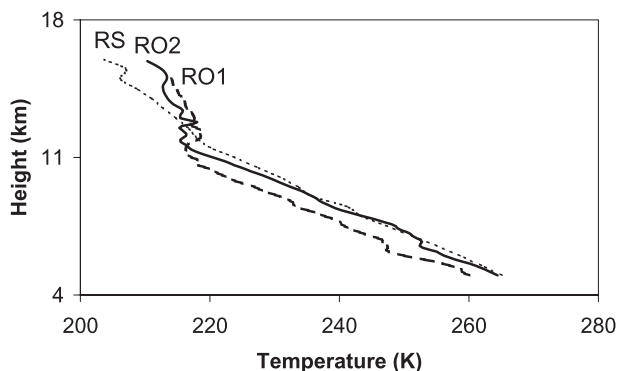


FIG. 3. Temperature profiles in terms of height between 5-km altitude and the tropopause. Soundings of the two GPS RO and the balloon on 3 Nov 2006 were all close in distance and time.

from another technique (see below). However, the filtering windows of the observational methods (Alexander 1998) must share at least some portion of the wavelength spectrum (otherwise they will not be able to see the same waves).

Then we tried a different combination of observational techniques. We first looked for the last 4 yr of radio soundings from El Plumerillo airport (32.8°S, 68.8°W) on the lee side of the highest Andes tops and then searched for each case if there were any two nearby in space and time GPS RO (with a relaxed criterion of proximity to 400 km). A triad was formed on 3 November 2006 with a radio sounding (RS) launched at 1200 UTC (the balloon ascent takes about 1 h) and two GPS RO from COSMIC (respectively RO1 and RO2) that occurred, respectively, at 1232 UTC (36.9°S, 69.4°W) and at 1410 UTC (33.2°S, 66.3°W). The temperature profiles in terms of the height may be seen in Fig. 3 between 5-km altitude (GPS RO soundings are more reliable above about this height because of significant humidity in the lower troposphere) and the tropopause (the considered balloon soundings usually reach this zone or may just enter the lower stratosphere). We first verified that the three trajectories satisfied the straight line sounding test. Then we detrended the three curves and tried to find in each of them any dominant wave by a sinusoidal fit with three parameters: amplitude, wavelength, and phase. We preferred to use this method instead of the Fourier technique because the latter results are restricted to the wavelengths that are an integer subdivision of the total length. In the present examples the slant trajectories cover a total distance about 40 km, which would then imply an uncertainty about 10% for an 8-km mode. We implicitly assumed that the dominant mode thus found in each sounding corresponded to the same wave. It must be recalled that the plots represent the observations along the sounding paths, which differ from the vertical direction, so the wavelengths along the

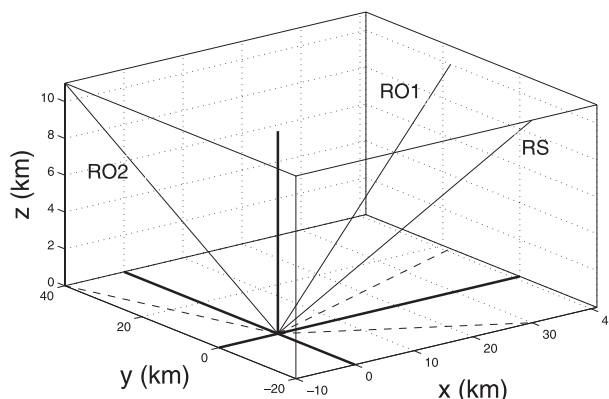


FIG. 4. The relative orientation of the three soundings, where the dashed lines represent their projection on the horizontal plane. Boldface lines show the three Cartesian axes. The three zenith angles and the three azimuth angles for RS, RO1, and RO2 are 73°, 77°, 75° and 326°, 24°, 104°, respectively. Notice that the vertical scale is quite different than the other two; the real configuration looks more slanted.

trajectories  $\lambda_i$  had to be calculated using the corresponding zenith angle of each path (73°, 77°, and 75°, respectively, for RS, RO1, and RO2). We obtained  $\lambda_1 = 6.6$  km (RS),  $\lambda_2 = 8.4$  km (RO1), and  $\lambda_3 = 7.8$  km (RO2). Reduced chi-square values of the fits were, respectively, 2.7, 1.8, and 1.9. Radio soundings may often yield nearly vertical trajectories (which is very favorable to form a triad with 2 RO), but this was not the case here, mainly because of the strong westerly winds above the Andes. Therefore, the three zenith angles were not very far from 90°. However, the azimuthal angles were well distributed, not stemming from nearly parallel trajectories: 326°, 24°, and 104° respectively for RS, RO1, and RO2 (angles measured counterclockwise from the east). The relative orientation of the three soundings in three dimensions is shown in Fig. 4. The condition number calculation led to a value of 5.6 [in fact, inequality (4) gives an upper bound estimation of 6], which has been marked in Fig. 2. From the three experiments, the radio sounding exhibited the largest uncertainties in the straight line fit, and these were used to calculate the error propagation to **A** and **b**, leading to  $\epsilon_{\mathbf{A}} = 2\%$  and  $\epsilon_{\mathbf{b}} = 6\%$ . Position errors for GPS RO and balloons are on the order of a few meters (Businger et al. 1996; Kursinski et al. 1997), so they will introduce uncertainties around 0.1% in distances of a few kilometers or angles derived from them. We obtained a 50% uncertainty bound in inequality (3). From the eight linear equation systems to be solved, only one solution complied with  $\lambda_x < 0$  and  $\lambda_z < 0$ , so no further requirement was necessary for  $\lambda_y$ . The values that were obtained are  $\lambda_x = 98$  km,  $\lambda_y = 713$  km, and  $\lambda_z = 2.0$  km (see Table 1 for a summary of measurements and results), which are quite representative of MW in this



TABLE 1. Summary of measurements and results in the computation of Cartesian wavelengths of a mountain wave from three close soundings.

	RS	RO1	RO2
$\lambda$	6.6 km	8.4 km	7.8 km
$\theta$	73°	77°	75°
$\phi$	326°	24°	104°
	$\lambda_x = 98$ km	$\lambda_y = 713$ km	$\lambda_z = 2.0$ km

region (de la Torre and Alexander 2005). The corresponding estimated errors in the computation of wavelengths are, respectively, 49, 357, and 1.0 km.

#### 4. Conclusions

Three atmospheric soundings in a given region and time interval do not guarantee that the three Cartesian wavelengths of MW can be inferred. The magnification of the input relative error of the detected wavelengths by propagation to the Cartesian wavelengths calculation depends strongly on the relative orientation of the three soundings and it is shown that an appropriate error upper bound may be found directly in each case. Three perpendicular soundings represent the ideal case. Any three close oblique experiments may have the problem that an almost orthogonal set may not be found, because none of them has at least a nearly vertical trajectory. However, if the three soundings are rather well distributed with respect to the azimuthal angle, then they may reach acceptable error limits. Also, two limb experiments may be combined with a third rather vertical technique, which may provide a nearly orthogonal set, that would imply a low uncertainty in the outcome. An ambiguity of more than one acceptable solution may not be avoided in some cases.

*Acknowledgments.* GPS RO data were downloaded from <http://www.cosmic.ucar.edu/>. Balloon data were obtained from Servicio Meteorológico Nacional. Authors P. Alexander and A. de la Torre are members of CONICET.

This work was supported by grants UBACYT X004, CONICET PIP 5932, and ANPCYT PICT 1999.

#### REFERENCES

- Alexander, M. J., 1998: Interpretations of observed climatological patterns in stratospheric gravity wave variance. *J. Geophys. Res.*, **103**, 8627–8640.
- Alexander, P., A. de la Torre, and P. Llamedo, 2008: Interpretation of gravity wave signatures in GPS radio occultations. *J. Geophys. Res.*, **113**, D16117, doi:10.1029/2007JD009390.
- Businger, S., S. R. Chiswell, W. C. Ullner, and R. Johnson, 1996: Balloons as a Lagrangian measurement platform for atmospheric research. *J. Geophys. Res.*, **101**, 4363–4376.
- de la Torre, A., and P. Alexander, 1995: The interpretation of wavelengths and periods as measured from atmospheric balloons. *J. Appl. Meteor.*, **34**, 2747–2754.
- , and —, 2005: Gravity waves above Andes detected from GPS radio occultation temperature profiles: Mountain forcing? *Geophys. Res. Lett.*, **32**, L17815, doi:10.1029/2005GL022959.
- Gill, A. E., 1982: *Atmosphere–Ocean Dynamics*. Academic Press, 662 pp.
- Golub, G. H., and C. F. V. Loan, 1996: *Matrix Computations*. The John Hopkins University Press, 694 pp.
- Guggenheimer, H. W., A. S. Edelman, and C. R. Johnson, 1995: A simple estimate of the condition number of a linear system. *Coll. Math. J.*, **26**, 2–5.
- Holton, J. R., 2004: *An Introduction to Dynamic Meteorology*. Elsevier, 535 pp.
- Kursinski, E. R., G. A. Hajj, J. T. Schofield, R. P. Linfield, and K. R. Hardy, 1997: Observing Earth's atmosphere with radio occultation measurements using the global positioning system. *J. Geophys. Res.*, **102**, 23 429–23 465.
- Liou, Y.-A., A. G. Pavelyev, S.-F. Liu, A. A. Pavelyev, N. Yen, C.-Y. Huang, and C. J. Fong, 2007: FORMOSAT-3/COSMIC GPS radio occultation mission: Preliminary results. *IEEE Trans. Geosci. Remote Sens.*, **45**, 3813–3826.
- Press, W. H., S. A. Teukolsky, W. T. Vetterling, and B. P. Flannery, 1999: *Numerical Recipes in Fortran 77: The Art of Scientific Computing*. Cambridge University Press, 976 pp.
- Preusse, P., A. Dörnbrack, S. D. Eckermann, M. Riese, B. Schaeler, J. T. Bacmeister, D. Broutman, and K. U. Grossmann, 2002: Space-based measurements of stratospheric mountain waves by CRISTA 1. Sensitivity, analysis method, and a case study. *J. Geophys. Res.*, **107**, 8178, doi:10.1029/2001JD000699.
- Shutts, G. J., P. Healey, and S. D. Mobbs, 1994: A multiple sounding technique for the study of gravity waves. *Quart. J. Roy. Meteor. Soc.*, **120**, 59–77.